Heliyon 6 (2020) e03750

Contents lists available at ScienceDirect

Heliyon

journal homepage: www.cell.com/heliyon

Research article

Novel nitrogen-doped carbon dots prepared under microwave-irradiation for highly sensitive detection of mercury ions

Ali Ghanem, Rama Al-Qassar Bani Al-Marjeh, Yomen Atassi *

Department of Applied Physics, Higher Institute for Applied Sciences and Technology, Damascus, Syria

ARTICLE INFO

Keywords:
Analytical chemistry
Environmental science
Carbon dots
Hg^{2+} detection
Photoluminescence
pH sensing
LOD

ABSTRACT

In this paper, new nitrogen doped carbon dots with a high quantum yield and novel optical properties were synthesized by a simple and fast one step microwave-assisted synthesis. Citric acid monohydrate was used as a carbon source and 2,2-dimethyl-1,3-propanediamine as nitrogen source. The prepared N-CDs were characterized by Fourier transform infrared, Raman, UV-visible and photoluminescence spectroscopies. Transmission electron microscope (TEM) images revealed that the N-CDs have distinctive flake-shape morphology. The N-CDs exhibit bright blue luminescence and quenching response towards Hg^{2+} ions. The quenching sensitivity was investigated. The results indicate a limit of detection as low as 7.63 nM and a linear relationship over the range 0–4.2 μM. In addition, the prepared N-CDs were tested as sensor for pH in the range from 1 to 7.

1. Introduction

Mercury is one of the most dangerous contaminants that poses serious risks to ecosystems and human health, even at low concentrations [1, 2]. There is no doubt that the pollution of aquatic ecosystems with mercury is the main way through which mercury is transferred to drinking water, food chains and then to humans [3, 4]. There are three oxidation states of mercury, Hg (0), Hg (I) and Hg (II). Among these states, bivalent ions Hg^{2+} are the dominant form in water because of their stability and high solubility [5, 6, 7]. Hg^{2+} can form methylmercury which has carcinogenic effect and can cause neural cell damage, acute renal failure, hematopoietic and cardiovascular toxicity [8, 9, 10, 11, 12]. Therefore, it is important to look for new analytical techniques and methods that enable us to detect effectively and efficiently mercury ions Hg^{2+} at the lowest detectable concentrations in order to prevent their poisoning [13]. There are many analytical methods used for this purpose, such as atomic absorption spectroscopy, surface enhanced Raman scattering, inductively coupled plasma mass spectrometry, cyclic voltammetry with electrochemical liquid-phase micro extraction and cold-vapor atomic absorption spectroscopy, but these methods need sophisticated instrumentation and critical sample preparation [13, 14, 15, 16, 17, 18, 19].

Fluorescence spectroscopy has received considerable attention from analytical chemistry researchers because of its advantages over the above - mentioned methods such as its high sensitivity, low cost and simplicity in performing the analysis [8, 20]. Many promising fluorescent materials that are sensitive to mercury ions have been developed such as organic fluorophores, metal nanoparticles, noble metal nanoparticles, fluorescent doped silica, semiconductor quantum dots, and recently carbon quantum dots (CQDs) [21, 22]. With the exception of CQDs, those substances have many disadvantages that limit their application for the purpose of detecting mercury ions, including toxicity and poor photostability. In addition, most of them are not ecofriendly [22].

In comparison with other materials, CQDs have many advantages that make them preferred in application owing to their low toxicity, unique optical properties, ease of preparation, possibility of surface modification, good photo-stability, and chemical stability [23, 24, 25]. CQDs were investigated as probes for detection of Fe^{3+}, Cu^{2+}, iodide ions, melamine, Nitrite ions, Dopamine, l-cysteine, tetracycline, and Hg^{2+} ions [1, 9, 24, 25, 26, 27, 28, 29, 30].

Furthermore, there are many other applications of CQDs, like bioimaging, catalysis, drug delivery, and pH sensing, to name a few [31, 32, 33]. On the other hand, determination of pH value is very important and critical for many fields including agronomy, biology, nutrition, water purification, and biology [34, 35, 36]. Some CQDs with special optical and structural properties show good pH sensitivity [37]. This sensitivity is still subject to further investigation with the aim of preparing effective CQDs from both inexpensive and safe carbon sources [38].

This study presents the preparation of novel nitrogen-doped carbon dots (N-CDs) by microwave-assisted method with a high quantum yield (QY) that reaches 51.2%. These N-CDs were characterized by appropriate

* Corresponding author.
E-mail address: yomen.atassi@hiast.edu.sy (Y. Atassi).

https://doi.org/10.1016/j.heliyon.2020.e03750
Received 9 February 2019; Received in revised form 1 February 2020; Accepted 2 April 2020

instruments and then investigated as a probe for the detection of mercury ions (Hg^{2+}) as well as their sensitivity to pH values. In order to assess the performance of the current N-CDs, their performance is compared with those of already published CDs.

2. Experimental

2.1. Materials

Citric acid monohydrate, 2,2-dimethyl-1,3-propanediamine (for synthesis) and quinine sulfate for quantum yield determinations were purchased from Sigma-Aldrich and used as received. All other reagents were analytical and also used without any further purification.

2.2. Instruments

Transmission electron microscopy (TEM) micrographs were performed on Tecnai F20 transmission electron microscope at accelerating voltages up to 200 kV. The Fourier transform infrared Spectroscopy (FTIR) spectra were measured by the infrared spectrophotometer (Bruker, Vector 22). X-Ray Diffraction pattern was obtained using (Philips, PW3710) diffractometer with Cu-K_α radiation ($\lambda = 1.54$ Å). Elemental analysis was conducted by vario MICRO elementar made by elementar Analysensysteme GmbH. UV-vis spectra were recorded using UV-vis spectrometer (JASCO, V-350). For Raman spectroscopy, Horiba spectrometer T64000 was utilized with excitation wavelength at 532 nm. The spectral measurements of fluorescence were performed on (JASCO, FP-8300) Spectrofluorometer. pH measurements were carried out by (TWT, pH7110) pH meter.

2.3. Preparation of the N-CDs

The nitrogen doped CDs were prepared using the microwave-assisted pyrolysis method as follows: 2.1 g (0.01 mol) of citric acid monohydrate and 1.02 g (0.01 mol) of 2,2-dimethyl-1,3-propanediamine were dissolved in a glass beaker containing 20 ml of distilled water. The mixture was stirred using a magnetic stirrer until a clear homogeneous solution was obtained. Then, the mixture was transferred to a domestic microwave and was irradiated at 570 W for 15 min. At the end of heat treatment, the water is evaporated and a brown solid was obtained. The obtained solid was dissolved in 25 ml of water and then filtrated. To evaporate the water, the solution was left at the laboratory temperature for seven days. Then the residue, consisting of N- CDs, is kept for further investigation.

2.4. Quantum yield calculation

The quantum yield of the prepared N-CDs was calculated using quinine sulfate dissolved in H_2SO_4 0.1 mol/L as a standard. Five different concentrations of both standard and samples were prepared. The absorbance measurements were conducted at the wavelength 360 nm, and kept below absorbance of 0.06. then the fluorescence spectra were measured at the same wavelength (360nm), and the area under the curve were integrated between 380 and 600 nm to obtain the energies of photoluminescence (PL). By plotting the absorbance versus photoluminescence energies. The quantum yield was calculated by the following Eq. (1) [4]:

$$\Phi_c = \Phi_s \times (m_c/m_s) \times \eta^2_c/\eta^2_s \quad (1)$$

(c refers to the N-CDs and S refers to standard), where Φ is the quantum yield (54% for quinine sulfate) [4], η the refractive index of the solvent (1.3 for water, and 1.33 for H_2SO_4 0.1 mol.L^{-1}) [13], m_c is the slope of sample plot and m_s is the slope of standard plot.

2.5. Spectrofluorometric detection of Hg^{2+} ions

The quenching response of the prepared N-CDs towards Hg^{2+} ions was investigated in phosphate buffer solution (PBS, pH = 7) at room temperature. Samples containing Hg^{2+} ions with precisely known concentrations were prepared. The Hg^{2+} ion detection test is performed according to this typical procedure: 1 ml of the N-CDS solution (0.2 g.L^{-1}) were added to a mixture of 8 ml phosphate buffer solution and 1 ml of Hg^{2+} ions with certain calculated concentration. After mixing for 10 min, the final mixture was left for two hours before measurements to ensure that the reaction was completed. The same procedure was also used for solutions of other ions (Na^+, Ca^{2+}, Mg^{2+}, Cr^{3+}, Co^{2+}, Mn^{2+}, Cu^{2+}, Zn^{2+}, Fe^{3+}, Al^{3+}, Pb^{2+}, Ni^{2+}, Ag^+, NH_4^+, Bi^{3+}) and for solutions containing a mixture of these ions. The fluorescence spectra of all solutions (blank, Hg^{2+}, metal ions, mixture of ions without Hg^{2+} and mixed ions with Hg^{2+}) were recorded at 360 nm excitation wavelength.

2.6. pH sensing procedure

For pH sensing procedure, several solutions of NaOH and HCl were used. The general procedure was conducted as follows: 1 ml of the N-CDs solution (0.2 g.L^{-1}) was added to 9 ml of acidic or alkaline solution with certain pH value. Then, fluorescence intensity was measured.

3. Results and discussion

3.1. Optimization of synthesis conditions

The N-CDs were prepared by one-step microwave-assisted method using citric acid as a source of carbon and 2,2-dimethyl-1,3-propanediamine as a source of nitrogen. The water evaporated during heating and the color of the formed solid gradually turned into brownish. At the end of the heat treatment, a solid brown material was obtained, indicating carbonization was occurred. The route of the synthesis is illustrated in Figure 1.

The synthesis is affected by many factors like the microwave power, the molar ratio and the irradiation time. Thus, to set the optimal conditions for synthesis which yield carbon dots with the best fluorescence properties, an optimization study was conducted. The optimal parameters were found to be: (1:1) molar ratio of carbon source to nitrogen source, the microwave power 570 W, and the irradiation time 15 min. The different optimizations of N-CDs synthesis parameters are illustrated in Figures 2, 3, and 4.

3.2. Morphological and structural characterizations of the N-CDs

Transmission electron microscopy (TEM) was used to characterize the morphology of the prepared N-CDs. TEM images (Figure 5A and B) show that the prepared N-CDs have flake-shape morphology and were consistently dispersed, and about 70% of the size distribution is in the range (40–60 nm) with a maximum population at 50 nm. The relatively large particle size has been already reported in the literature for other carbon dots (Cdots) [39, 40, 41].

Fourier-transform infrared spectroscopy (FTIR), as a common technique for identifying surface functional groups of materials, was used for further characterization of the prepared N-CDs. Figure 6-A represents the IR spectrum of the N-CDs.

The broad absorption band at around 3345 cm^{-1} refers to the stretching vibrations of the O–H/N–H groups which play an important role in enhancing the solubility of the N-CDs [24, 42, 43, 44, 45]. The shoulder band at 2950 cm^{-1} is attributed to the stretching vibration of C–H [42, 46]. The bands at 1710 cm^{-1}, 1560 cm^{-1} and 1300 cm^{-1} correspond to C=O and C=C and C–O stretching vibrations, respectively [46, 47, 48]. In addition, the band at 1390 cm^{-1} is related to C–N in amide, whereas the band at 1150 cm^{-1} is ascribed to C–N stretching in amine and confirms the presence of amine group on the surface of N-CDs

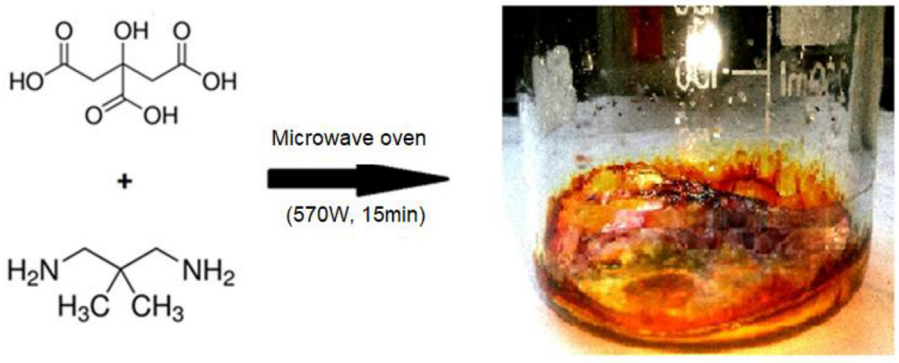

Figure 1. Synthesis route of the N-CDs.

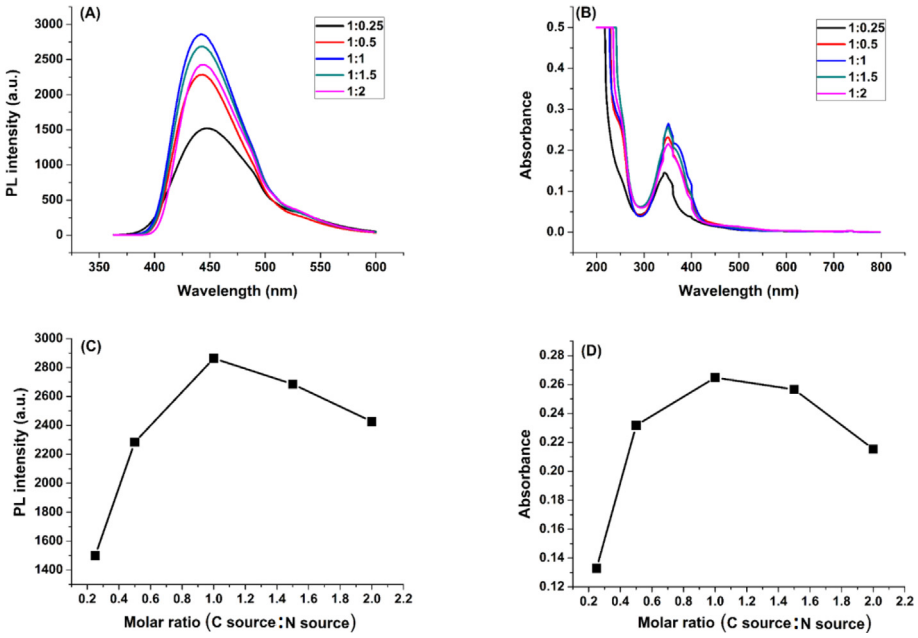

Figure 2. Optimization of C source:N source molar ratio parameter, (A) and (B): Fluorescence and UV-vis spectra of N-CDs, respectively, at various C: N molar ratios, (C) and (D): Fluorescence intensity and Absorbance, respectively, as a function of C: N molar ratios.

[46, 47, 48, 49, 50]. Furthermore, a distinctive band was observed at 1652 cm^{-1}, which represents a typical stretching mode of aromatic C=N [48]. The results obtained from IR spectrum analysis confirm that the used diamine is grafted on the surface of the carbon dots and amidation reaction should have occurred. Moreover, IR spectra showed a variety of surface groups that lead to fluorescence and also contribute to chemical and optical stability. The results also suggest that nitrogen atoms could be present at the structure of the prepared N-CDs as amine and amide groups, and can be present in the core of the N-CDs as aromatic structure, which may explain their role in enhancing the fluorescence.

For more detailed structural and compositional information about the N-CDs, elemental analysis was carried out for the N-CDs prepared according to the optimum conditions, and the result was as follows: C: 62.55%, H: 9.140%, N: 14.44%, and O: 13.87% (calculated). The result indicates that the as-prepared N-CDs have nitrogen-rich structure.

X-ray diffraction pattern was obtained in the range between 10 to 80°. Figure 6-B shows that the N-CDs have broad diffraction peak at 19.25°. This peak corroborates the amorphous nature of the N-CDs.

Raman spectrum of N-CDs recorded with 532 nm excitation wavelength is shown in Figure 7. Raman spectrum shows two distinct peaks at 1370 (D-band) and 1602 cm^{-1} (G-band), respectively. The G-band (sp^2 hybridization) is related to the amount of graphitization associated with the N-CDs, whereas D-band (sp^3 hybridization) is linked to defects and functionalization [51, 52]. The intensity ratio of the peak of the G band to the D band was found to be 1.71 [53]. The higher G/D ratio indicates that the synthesized N-CDs are mostly composed of graphitic structure with a certain number of defects and functionalization of N-CDs [54, 55].

3.3. Optical properties of the NCDs

To investigate the optical properties of the N-CDs, UV-vis absorption spectra and fluorescence spectra of aqueous solutions were recorded. Typically, UV-vis spectroscopy is used to evaluate the maximum absorption by CQDs and thus to set the excitation wavelength at which the emission is maximum in order to obtain the best fluorescence. Two absorption bands are observed in the UV-vis spectrum (Figure 8 - A) of the N-CDs aqueous solution. The shoulder at 250 nm is attributed to π-π^* transitions in C=O, C=C and C=N [13, 42, 48, 56]. The other maximum at 360 is ascribed to the typical n-π^* transitions in carbonyl bond C=O [48, 56]. The prepared N-CDs have unsaturated bonds which contain nitrogen atom. Introducing doping heteroatoms (e.g., nitrogen, boron, sulfur or phosphorus) endows the carbon dots with electron-rich nature that results in easier energy transfer to the excited π^* of the sp^2 orbitals, and eventually enhances the fluorescence [13].

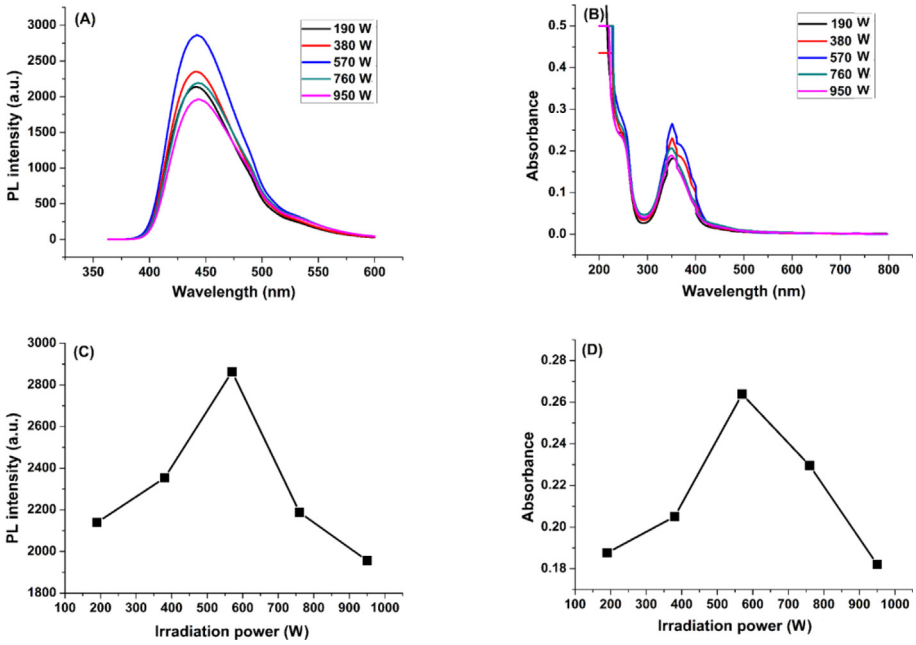

Figure 3. Optimization of microwave irradiation power parameter: (A) and (B): Fluorescence and UV-vis spectra of N-CDs, respectively, at various microwave irradiation power, (C) and (D): Fluorescence intensity and Absorbance, respectively, as a function of microwave irradiation power.

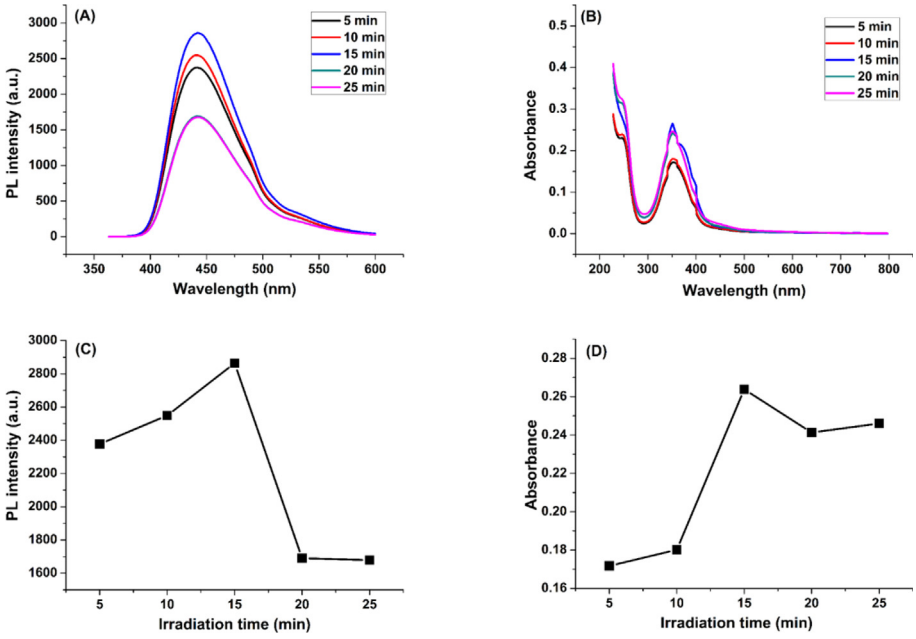

Figure 4. Optimization of irradiation time parameter: (A) and (B): Fluorescence and UV-vis spectra of N-CDs, respectively, at various irradiation times, (C) and (D): Fluorescence intensity and Absorbance, respectively, as a function of irradiation time.

Figure 8 – B shows the excitation and emission spectra of the N-CDs. The detailed fluorescence spectra of the N-CDs at various excitation wavelengths (from 300 to 400 nm, with increment of 10 nm at every step) are shown in the (Figure 8C). The highest fluorescence intensity at 440 nm was obtained by the excitation wavelength at 360 nm, and no obvious shift was observed in the fluorescence peak at 440 nm of the recorded spectra in the range between 300 nm and 400 nm. So, the prepared N-CDs exhibit typical excitation-independent feature. The N-CDs solution emits very bright blue luminescence under UV lamp (365 nm) as can be seen in the inset of (Figure 8B). Quantum yield was calculated using quinine sulfate as a standard material. The prepared N-CDs have a high quantum yield that reaches about 51.2% (Figure 8D).

3.4. Photostability of the N-CDs

To investigate the stability of the prepared N-CDs, three factors affecting the fluorescence were studied: the effect of exposure to ultraviolet light, the effect of ionic strength and the effect of pH.

The N-CDs solution was exposed continuously to ultraviolet light from a lamp at a wavelength of 365 nm for different periods of time: 5, 10, 15, 20, 25, and 30 min. The results indicate that there is no significant change in the intensity of fluorescence during these periods of time as seen in (Figure 9 - A), where F_0 and F are the fluorescence intensities at 440 nm, under excitation at 360 nm, without NaCl and with NaCl, respectively.

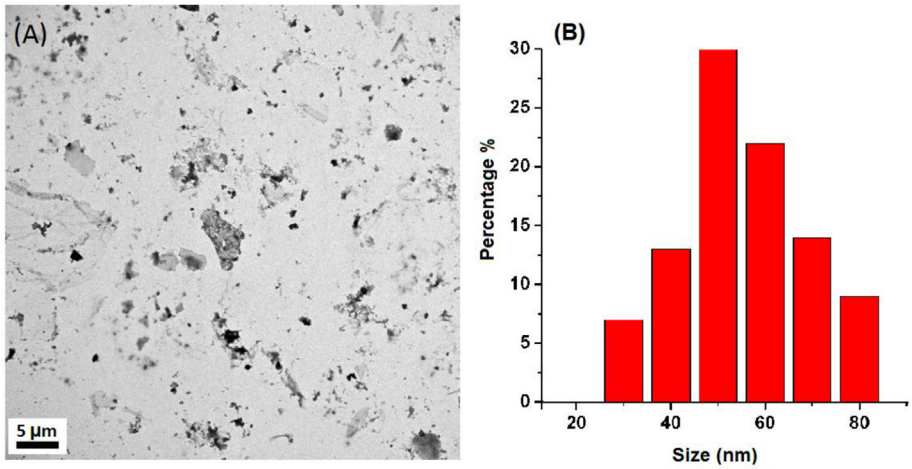

Figure 5. (a) TEM image of the prepared N-CDs and B) Size distribution of the N-CDs.

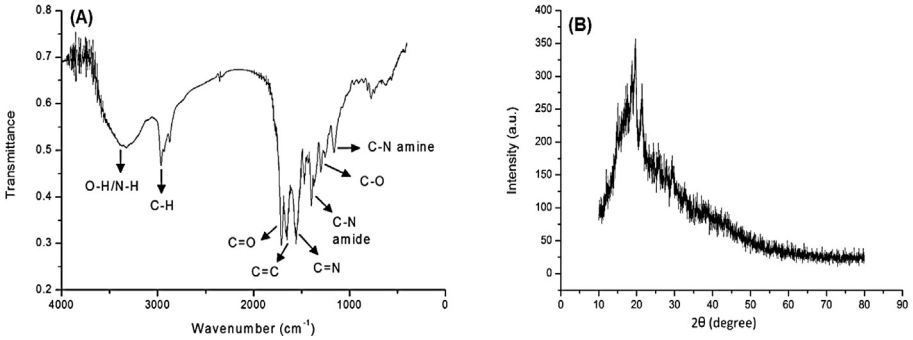

Figure 6. A) FTIR spectrum of the prepared N-CDs, B) X-ray diffraction pattern of the N-CDs.

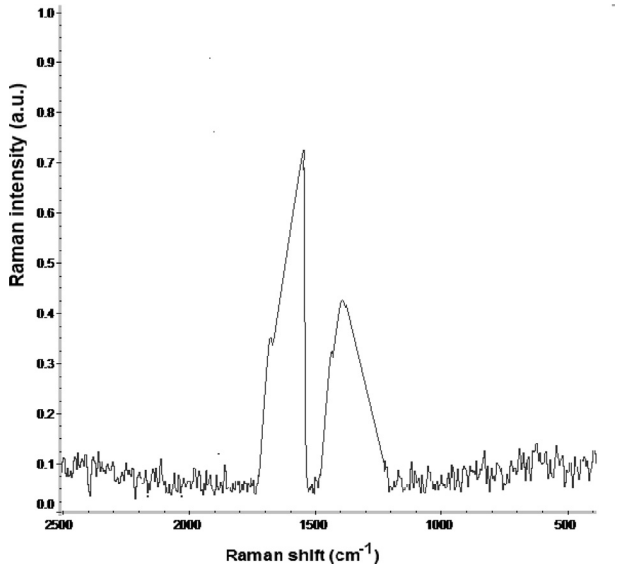

Figure 7. Raman spectrum of the prepared N-CDs with excitation wavelength of 532 nm.

The effect of ionic strength was studied by preparing six solutions of the N-CDs with various concentrations of NaCl. The fluorescence intensity remains unchanged up to 4 mol.L^{-1}. This demonstrates the non-dependence of the fluorescence of the prepared N-CDs on the solution ionic strength even at high concentration of NaCl (Figure 9 - B).

Generally, pH plays an important role in the emission intensity of CDs as their surface carries many functional groups that are affected by changes in the pH values. The pH effect was investigated in the range from 1 to 12. As shown in (Figure 9 - C), the fluorescence intensity is affected by pH values, especially for 1acidic pH. Effect of pH can be demonstrated by the role of surface groups. This point was studied in details later. It is clear that the best fluorescence was obtained at pH 7. So, the pH was fixed at this value during the spectrofluorometric detection experiments.

Furthermore, to ensure the photostability of the CDs for long time storage at room temprature, the flouescence intensity of stored CDs solution was measured periodically after 1,2,3 and four months. The measurements confirm the resistance of CDs to quenching during storage (Figure 9 - D).

3.5. Selectivity of the N-CDs towards Hg^{2+}

Owing to their unique optical properties, high stability towards a wide range of chemical environments and their solubility in various solvents, especially water, CQDs can be applied as probes for detection of metal ions [9, 24, 57]. The detection mechanism, mostly based on fluorescence quenching, depends on several factors. Among these factors, functional surface groups play a critical role by forming complexes with the target ions selectively [30, 57]. The use of CQDs in ions detection requires-as other analytical methods do-high selectivity. In fact, selectivity is a critical parameter to confirm the effectiveness of the detection procedure and to ensure that there is no interference between the target ion and other ions. To investigate the selectivity of the N-CDs towards mercury ions, solutions of representative ions were prepared including: Na^{+}, Ca^{2+}, Mg^{2+}, Cr^{3+}, Co^{2+}, Mn^{2+}, Cu^{2+}, Zn^{2+}, Fe^{3+}, Al^{3+}, Pb^{2+}, Ni^{2+},

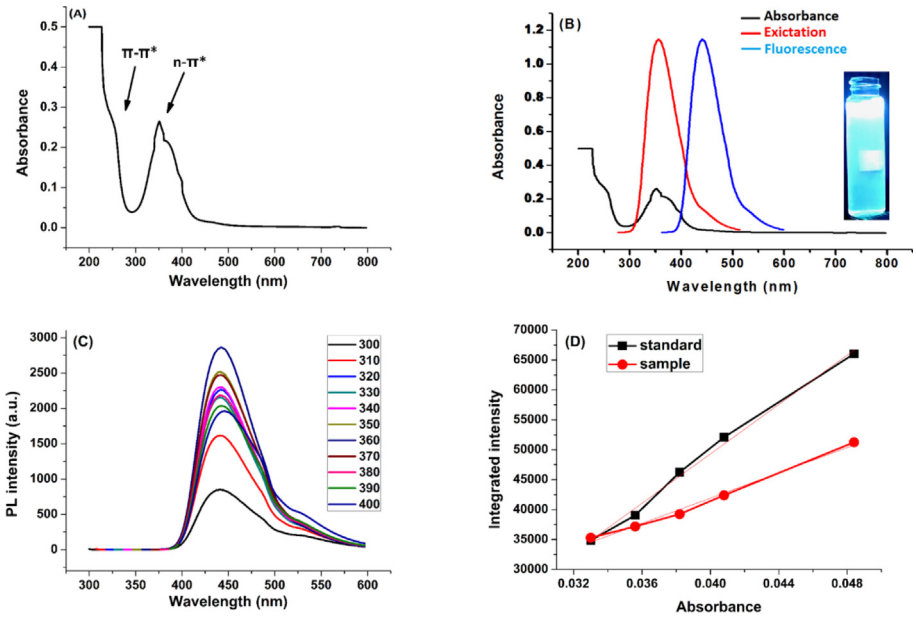

Figure 8. A) UV-vis spectrum of the N-CDs with two absorbance bands at 250 nm and 360 nm, B) Excitation and emission spectra of the N-CDs, C) Fluorescence spectra of the N-CDs at several excitation wavelengths, D) Quantum yield calculation by slope method.

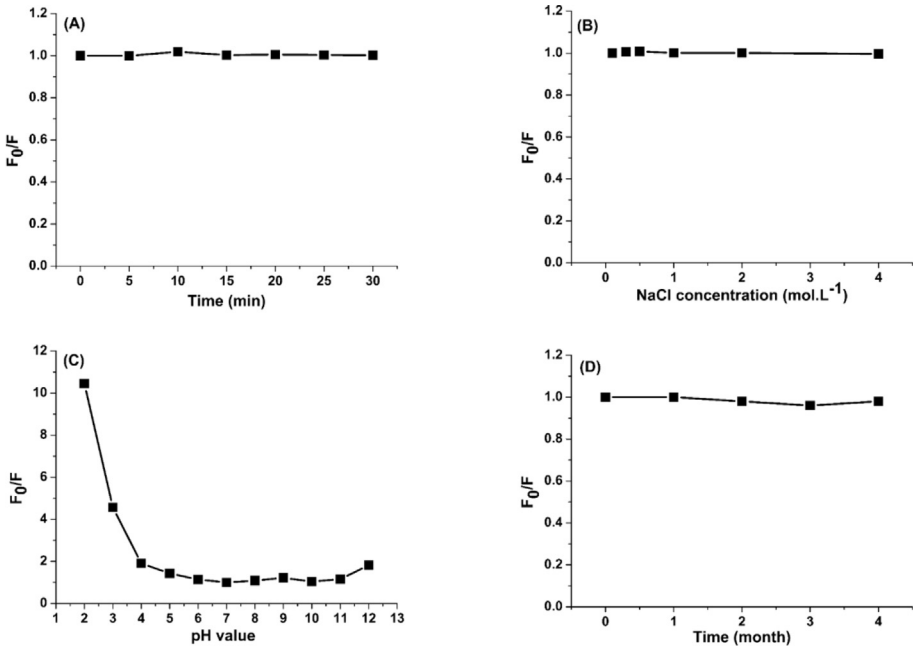

Figure 9. A) Effect of UV light on the fluorescence intensity for 30 min, B) Effect of the ionic strength (NaCl solution) on the fluorescence using different concentrations of the NaCl solutions till 4 mol.L^{-1}, C) The fluorescence intensity under effect of acidic and alkaline solutions, D) The effect of storage time on the fluorescence intensity.

Ag^{+}, NH_4^{+},Bi^{3+} and Hg^{2+} ions with concentration 24 μmol.L^{-1} for each ion and then the response of the N-CDs towards them were monitored by fluorescence measurements. For further investigation, we prepared a solution of a mixture of the ions without Hg^{2+}, and another one with a mixture of the ions in presence of Hg^{2+} ions, to study their competitive effect and to determine the mercury ions role in this response. Most of added ions to N-CDs, other than Hg^{2+}, do not exhibit a significant effect on the fluorescence spectrum. Some metal ions (such as Ag^{+} and Cu^{2+}) decreases the fluorescence intensity slightly, but this decrease is not a considerable interference (Figure 10 - A). In contrast, an obvious and significant decrease in spectrum intensity was observed for mercury ions (Figure 10 - A). In addition, the solution of mixed ions without Hg^{2+} does not cause quenching of the fluorescence intensity. On other hand, the fluorescence is sharply quenched in the presence of Hg^{2+} ions (Figure 10B,C). These results confirm that the prepared N-CDs are very sensitive and selective toward Hg^{2+}. This allows to implement the use of N-CDs as a probe in the practical detection of Hg^{2+} ions. Figure 10 - D shows a photographic image of N-CDs solution containing different metal ions, irradiated by UV lamp at wavelength 365 nm. It illustrates the naked-eye quenching response toward Hg^{2+} ions.

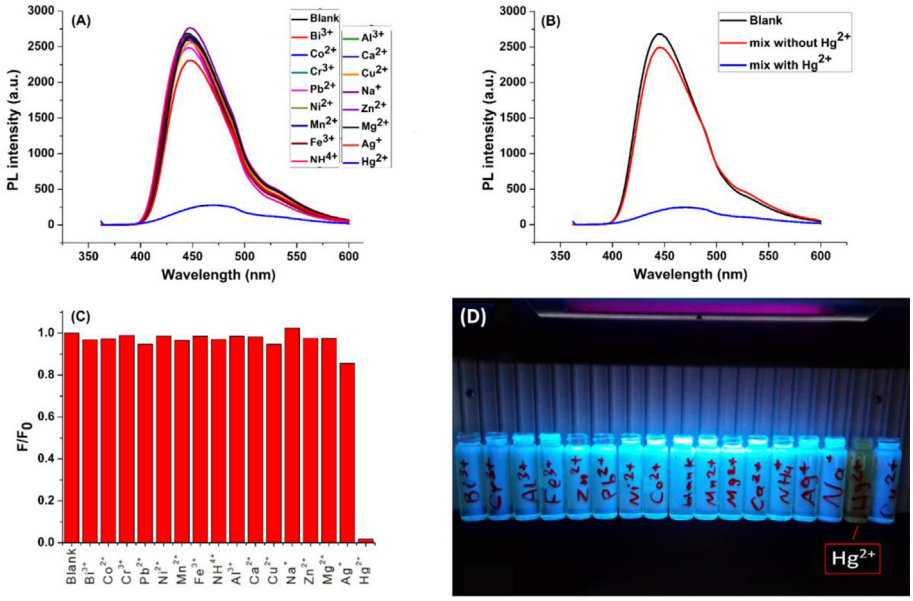

Figure 10. A) Response of the N-CDs towards several ions inclding Hg^{2+} ions, B) Effect of mixed ions with and without Hg^{2+} on the fluorescence intensity, C) Bar chart of (F/F_0) for every ion where F is the fluorescence of the N-CDs and ion mixture while F_0 refers to the fluorescence intensity of the blank N-CDs solution,D) Photographic image of the N-CDs solutions containing several ions under UV lamp irradiation at 365 nm.

3.6. Sensitivity of Hg^{2+} detection

The selectivity experiments show high selectivity of the N-CDs solutions toward Hg^{2+} ions, so further and systematic investigation was conducted to examine the response range which can be applied successfully for real determination of Hg^{2+} concentration. The concentration of the N-CDs solution was fixed at 0.02 $g.L^{-1}$ (as final concentration) and pH value is kept at 7 using PBS solution. Series of Hg^{2+} concentrations (from 0 to 24 μmol/L) were prepared by adding 1 ml of Hg^{2+} ions solution with calculated concentration to 8 ml of PBS solution and 1 ml of the N-CDs solution (0.2 $g.L^{-1}$), then the fluorescence spectra were measured (after two hours) to evaluate the quenching by comparing the sample spectra with the N-CDs blank solution spectrum. As shown in the (Figure 11 - A), it is observed that fluorescence intensity gradually decreases with the increasing concentration of Hg^{2+} ions and the fluorescence is fully quenched at Hg^{2+} concentration 24 μmol. Moreover, it is observed that higher concentrations cause red shift that reaches 33 nm at Hg^{2+} concentration 24 μmol/L.

For detailed investigation, we plotted Hg^{2+} ions concentrations (from 0 to 24 μmol/L) versus F_0/F (where F_0 and F are the fluorescence intensity at 440 nm, under excitation at 360 nm, without Hg^{2+} and with Hg^{2+} at determined concentration, respectively) and a good linear correlation ($R^2 = 0.998$) is obtained in the range between 0 and 4.2 μmol (Figure 11 – B, C). The limit of detection (LOD) was calculated to be 7.63 nM using Eq. (2) [13]:

$$LOD = 3\sigma/s \quad (2)$$

(σ represents the standard deviation and s refers to the slope of the linear fit).

It is notable that the linear behavior of quenching could be fitted with Stern-Volmer Eq. (3) [4]:

$$\frac{F_0}{F} = 1 + K_{SV}C \quad (3)$$

K_{sv} is the quenching constant, and C is the corresponding concentration of Hg^{2+} ions. Stern-Volmer equation for the current study is: $F_0/F = 1.67 [Hg^{2+}] + 1.01$.

To explain this behavior, many points must be taken into account. First of all, complexation interaction between the N-CDs and Hg^{2+} ions may take place because of the presence of carboxyl, hydroxyl and amine groups on the N-CDs surface which have tendency to form coordination structures with Hg^{2+}, and the results of selectivity experiments reveal that these structures are more stable than those formed with other ions (especially Ag^{+} an Cu^{2+} ions) and as a result, the stability constants of complexes between Hg^{2+} ions and N-CDs are higher than those of other examined ions. Furthermore, the coordination complexes may result in a non-radiative electron transfer from the excited state of N-CDs particles to Hg^{2+}, thus leading to quenching of the fluorescence. The fluorescence and UV-vis spectra of the N-CDs blank and the N-CDs/Hg2+ mixture are depicted in (Figure 12-A, B). The comparison between the UV-vis spectra of blank N-CDs and N-CDs with Hg^{2+} ions (Figure 12-B) shows a red shift which suggests that the formed coordinated structures have changed their electronic distribution [13, 46, 58, 59, 60].

3.7. The gist behind the N-CDs selectivity towards Hg^{2+} with a high sensitivity

It is now well established that the nature of precursors plays a major role in determining carbon dots selectivity towards metal ions [61, 62, 63]. In a work published recently, the chelation with Hg(II) was attributed to the surface functional groups formed on the Cdots by hydrothermal heating of glucose, aspartic acid, and a branched polyethyleneimine [61]. In order to examine the effects of the three precursors on the formation of the surface chemistry of Cdots, each pair of the precursors was tested separately by forming Cdots and examined with metal ions. The authors showed how the selectivity had changed accordingly. None of the prepared Cdots were selective to Hg(II) ions alone, whereas some of them became selective and specific towards copper ions.

Herein, the inherent structure of both 2,2-dimethyl-1,3-propanediamine and citric acid precursors along with the preparation method parameters dictate the surface chemistry of the as-prepared N-CDs. Thus, the selectivity towards Hg(II) ions becomes an intrinsic property of the current N-CDs.

For more in depth understanding of the selectivity of the current N-CDs towards Hg^{2+} ions and the quenching mechanism, recovery of the fluorescence was investigated using chelating agents that have high binding affinity to Hg^{2+} ions, such as iodide ions I^{-}. Suitable volumes of

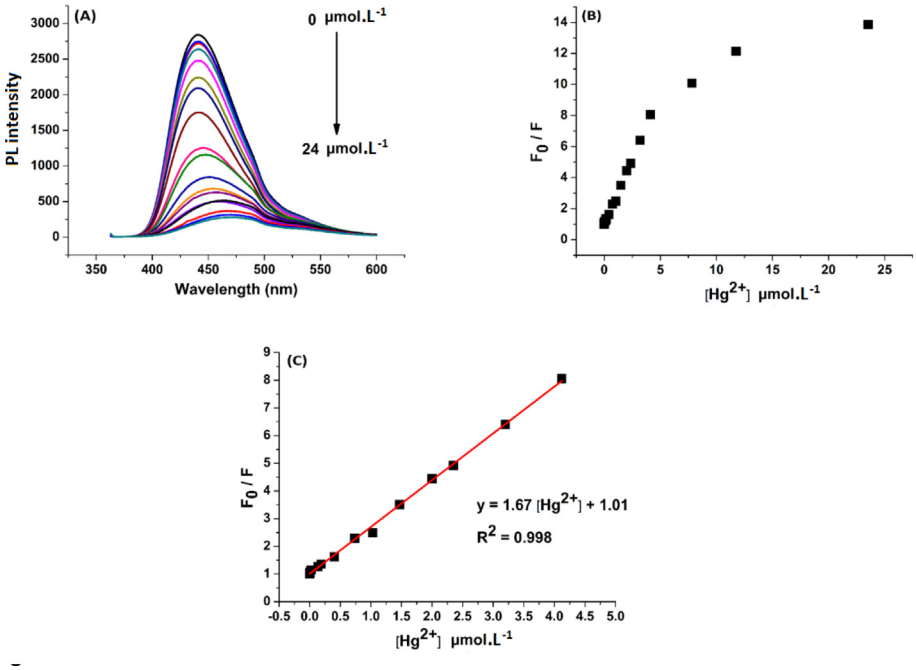

Figure 11. A) Fluorescence quenching in the presence of Hg^{2+} ions, B) Fluorescence quenching as function of Hg^{2+} ions concentration, C) The linear relationship between fluorescence quenching and Hg^{2+} ions concentration.

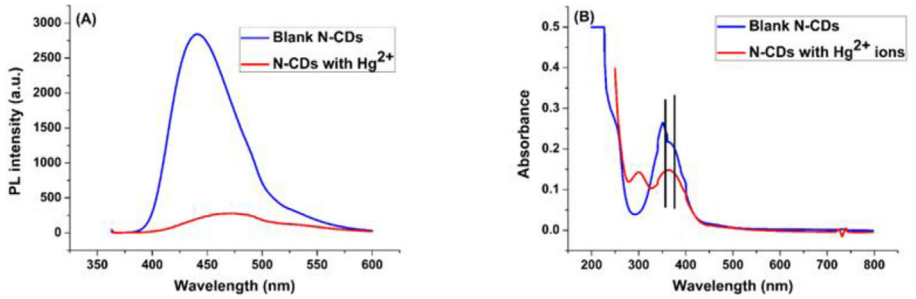

Figure 12. A) Comparison between fluorescence spectra of the N-CDs blank and the N-CDs/Hg^{2+} mixture, B) The red shift in the UV-vis spectrum of CDs/Hg^{2+} mixture in comparison with N-CDs blank.

iodide solution were added to Hg^{2+}/N-CDs system to get final concentrations in iodide ions ranging from 0 to 28 µmol/L. It was observed that the fluorescence intensity is recovered instantly by increasing I^- concentration and reached about 75% when I^- ions concentration was 28 µmol/L (Figure 13 – A).

It is known that the fluorescence of carbon dots is based on the radiative electron-hole recombination under excitations [63]; and according to this fact, a quencher such as Hg^{2+} can cause quenching by non-radiative electron/hole recombination/annihilation via an effective photo induced electron transfer process [62]. When adding Hg^{2+} to N-CDs solution, the affinity between Hg^{2+} ions and the functional groups

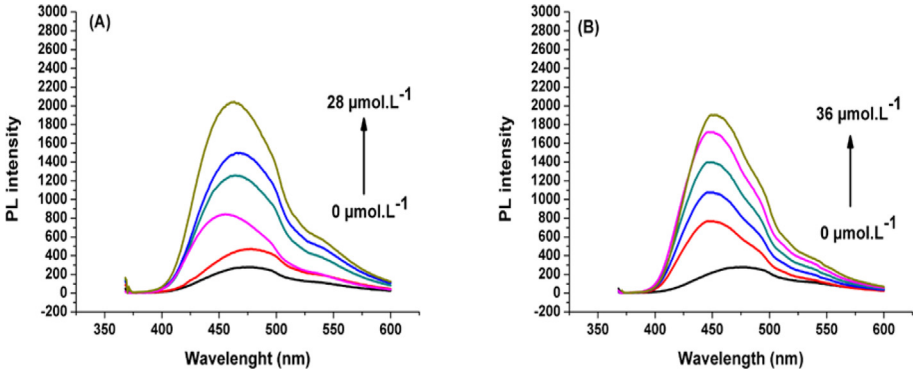

Figure 13. A) Fluorescence recovery of the Hg^{2+}/N-CDs complexes upon addition of increasing concentrations of I^- and B) Fluorescence recovery of the Hg^{2+}/N-CDs complexes upon addition of increasing concentrations of EDTA.

Table 1. Comparison of probe performance of the current N-CDs towards Hg^{2+} detection with other recent CDs.

Probe	Quantum yield (QY %)	Limit of detection (LOD)	Linear range	Year	Ref.
GQDs	15.4	0.439 nM	1–50 nM	2015	[64]
S,N-CDs	21.03	25 nM	0–15 μM	2016	[22]
N-CDs	42.2	83.5 nM	0–18 μM	2017	[8]
S,N-GQDs	41.9	0.14 nM	0.1–15 μM	2017	[65]
N-CDs	67	0.65 μM	0.001–5 μM	2018	[66]
N-CDs	40	20 nM	0–24 μM	2018	[1]
S,N-CDs	19.2	62 nM	0.1–20 μM	2018	[4]
N-CDs	————	38 ppb	0.12–2.0 ppm	2019	[41]
N-CDs	11.26	6.2 nM	0.001 μM (1 nM) to 8 μM	2019	[67]
N-CDs	51.2	7.63 nM	0–4.2 μM	2018	current work

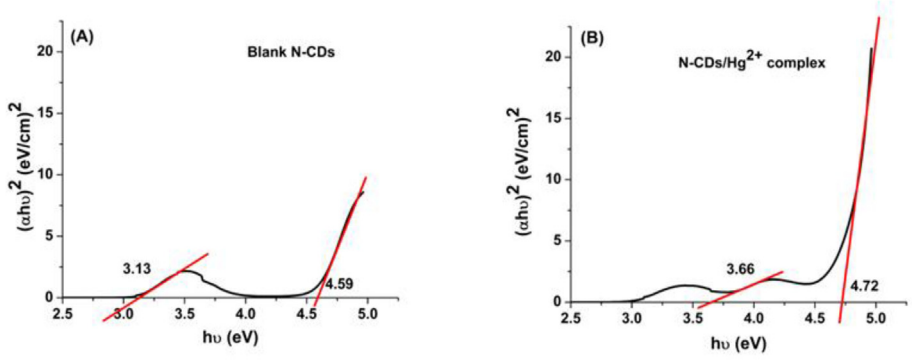

Figure 14. A) Band gap of blank N-CDs, B) Band gap of N-CDs/Hg^{2+} ions complex.

Table 2. Analysis results of detection of Hg^{2+} in tap water via spectrofluorimetric detection procedure.

Sample	Hg^{2+} Added (μmol)	Detected (μmol)	Recovery (%)	RSD (%)
1	0.25	0.248	99.2	1.22
2	0.8	0.805	100.6	1.63
3	1.5	1.480	98.6	0.88
4	3	2.940	98	1.46

of N-CDs (such as amines) leads to electrons transfer from the excited state of N-CDs to the empty d orbitals of Hg^{2+} ions, resulting in fluorescence quenching. The strong binding affinity between Hg^{2+} ions and I^- ions to form stable ion complex $[Hg\ I_4]^{2-}$ (complex formation constant $K_f([Hg\ I_4]^{2-}) = 1.9 \times 10^{30}$) leads to extracting Hg^{2+} ions from the complex (Hg^{2+}/N-CDs), getting free N-CDs and recovering the fluorescent emission [2]. In order to verify this assumption, the same procedure was repeated using EDTA ions (Y^{4-}) as chelating agent of Hg^{2+} instead of iodide ions. Y^{4-} ions are known to have lower binding affinity towards Hg^{2+} ions compared with I^- ions and consequently they form relatively less stable ion complex $[Hg\ Y]^{2-}$(complex formation constant $K_f([Hg\ Y]^{2-}) = 1.0 \times 10^{21.5}$).It was noticed that the prepared N-CDs restore to a lesser extent the fluorescence and recovered only about 60% of the photoluminescence intensity (vs 75% for I^-) at concentration of 28 μmol/L. Even at a higher Y^{4-} concentration of 36 μmol/L, only 68% of fluorescence is recovered (Figure 13– B). The abovementioned experiments shed light on the nature of quenching mechanism. The competition between different ligands to form stable complexes with Hg^{2+} could be the reason for the recovery of fluorescence emission.

Increasing the sensitivity by lowering the limit of detection is always a challenge in environmental trace analysis and analytical chemistry. It is well accepted that fluorescence-based analysis is one of the most sensitive technique for metal ion detection. Parameters such as fluorescence quantum yield and the selectivity towards a quencher are among the main factors that determine the sensitivity. By tailoring the design of carbon dots to obtain higher fluorophore quantum yield and greater selectivity towards a quencher, the limit of detection decreases and the detection method becomes more sensitive.

Promoting the fluorescence in Cdots is until now not sufficiently comprehended in literature, and it is considered as an open debate among specialists in the field. This is due to the variety of the Cdots and the complex nature of their formation. However, it is admitted that their surface functionalization through appropriate choice of precursors plays a primordial role in tuning their physiochemical properties. This results in tuning surface-related electronic levels in relation to energy levels of a particular metal ion (the quencher) [61].

In this respect, many preliminary experiments have been performed by our group to choose the best amine precursor that yields both the highest fluorescence quantum yield and the greatest selectivity towards Hg^{2+} ions. It has been proved that 2,2-dimethyl-1,3-propanediamine is the most appropriate precursor for the current experimental preparation method as it provides the adequate surface functionalization to have high detection sensitivity.

Table 1 contains a comparison between performance of the current N-CDs probe and other recent CQDs probes.

To understand the effect of Hg^{2+} ions from an energy perspective, the band gap values of the N-CDs and the N-CDs/Hg^{2+} complexes are evaluated. The band gaps were calculated using Tauc Eq. (4) [68]:

$$\alpha h\upsilon = k\left(h\upsilon - E_g\right)^n \times 100 \quad (4)$$

where $h\upsilon$ is the energy of exciting light, α is absorption coefficient and E_g is the band gap. We plotted $(\alpha h\upsilon)^2$ as a function of $h\upsilon$ (n = 1/2 for direct transitions). Figure 14 illustrates that two band gaps were observed at 3.13 eV and 4.59 eV for the N-CDs, and at 3.66 eV and 4.72 eV for the N-CDs/Hg^{2+} complex. These results suggest that Hg^{2+} ions cause higher

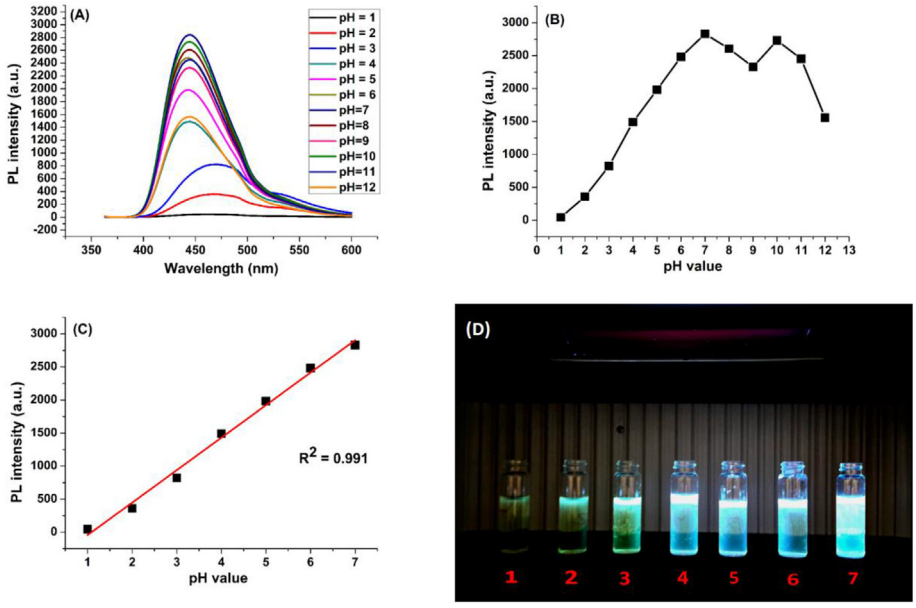

Figure 15. A) Fluorescence spectra of the prepared N-CDs in pH range between 2 and 12, B) Fluorescence spectra as function of pH value, C) The linear relationship between fluorescence and pH value in the range between 1 and 7, D) Photographic image of the N-CDs solutions at pH values from 1 to 7.

band gap when they coordinate with N-CDs. As a result, this will render electron transition harder, and lower the fluorescence intensity, i.e. induces fluorescence quenching.

3.8. Practical applications of the N-CDs for tap water

Photostability, selectivity, and sensitivity results indicate that the prepared N-CDs could be used for practical applications. So, the current fluorescence probe is applied for Hg^{2+} detection in tap water samples. Four samples taken from water tap were investigated by adding known concentrations of Hg^{2+} (0.25, 0.8, 1.5, 3 μmol.L^{-1}) according to the procedure described above (section 2.5.). Table 2 depicts the analysis results which confirm the effectiveness and accuracy of detection with relative standard deviation (RSD) lower than 2%.

3.9. pH sensing application

In addition to fluorescence quenching behavior of the N-CDs towards mercury ions and their quantitative application, they show a distinguishing response to pH values in acidic medium. The functional surface groups play a key role in this response owing to their protonated and non-protonated forms, especially carboxyl and amine groups. As shown in (Figure 15 – A) a red shift was observed in strong acidic pH values. As appeared in (Figure 15 – B, C), the fluorescence increases gradually in the range between 1 and 7, and a linear relationship is found by plotting the fluorescence intensity versus pH values ($R^2 = 0.991$). The effect of pH on the fluorescence of the N-CDs can be linked to the role of surface carboxyl, amino and amide groups. In acidic pH, the surface carboxyl groups may be protonated, and that leads to aggregation by hydrogen bonds and decrease of the fluorescence intensity [45, 59]. On the other hand, amino moieties may be protonated to form ($-NH_3^+$) which has important passivation effect [45]. Moreover, the critical role of amide group is attributed to extensive protonation-deprotonation according to which the deprotonated state has higher efficient electron donating property. Figure 15 – D shows a photographic image of the N-CDs solutions at pH values from 1 to 7, with different colors ranging from green to blue. In summary, these effects result in changing fluorescence with solution pH and shows a good sensing towards pH changes with excellent linearity that allows the applications of the current N-CDs in many fields, especially in biological applications.

4. Conclusion

In the present work, novel N-CDs by a one-step microwave-assisted synthesis were prepared. The prepared N-CDs have high quantum yield that reaches 51.2% and have been successfully applied for both: Hg^{2+} detection and pH sensing, where the obtained limit of detection for Hg^{2+} was as low as (7.63 nM) and the pH sensing covered a wide range from 1 to 7.

Declarations

Author contribution statement

Ali Ghanem: Conceived and designed the experiments; Performed the experiments; Analyzed and interpreted the data; Contributed reagents, materials, analysis tools or data; Wrote the paper.

Rama Al Qassar: Conceived and designed the experiments; Performed the experiments; Contributed reagents, materials, analysis tools or data.

Yomen Atassi: Conceived and designed the experiments; Analyzed and interpreted the data; Wrote the paper.

Funding statement

The authors would like to thank the Higher Institute for Applied Sciences and Technology (Syria) for providing funding to perform the current research under postgraduate research fellowships.

Competing interest statement

The authors declare no conflict of interest.

Additional information

No additional information is available for this paper.

References

[1] A. Iqbal, K. Iqbal, L. Xu, B. Li, D. Gong, X. Liu, Y. Guo, W. Liu, W. Qin, H. Guo, Heterogeneous synthesis of nitrogen-doped carbon dots prepared via anhydrous citric acid and melamine for selective and sensitive turn on-off-on detection of Hg

(II), glutathione and its cellular imaging, Sensor. Actuator. B Chem. 255 (2018) 1130–1138.
[2] F. Zahir, S. Rizwi, S. Haq, R. Khan, Low dose mercury toxicity and human health, Environ. Toxicol. Pharmacol. 20 (2005) 351–360.
[3] Y. Date, A. Aota, S. Terakado, K. Sasaki, N. Matsumoto, Y. Watanabe, T. Matsue, N. Ohmura, Trace-level mercury ion (Hg2+) analysis in aqueous sample based on solid-phase extraction followed by microfluidic immunoassay, Anal. Chem. 85 (2013) 434–440.
[4] R. Tabaraki, N. Sadeghinejad, Microwave assisted synthesis of doped carbon dots and their application as green and simple turn off–on fluorescent sensor for mercury (II) and iodide in environmental samples, Ecotoxicol. Environ. Saf. 153 (2018) 101–106.
[5] Z.S. Fernández, M.S. Quirós, M.C.C. Mj, M.R. Olivas, Development of a thiourea derivative polymer combined to a Direct Mercury Analyser for screening and pre-concentration of mercury species, Talanta 126 (2016) 612–617.
[6] G. Guzzi, C. La Porta, Molecular mechanisms triggered by mercury, Toxicology 244 (2008) 1–12.
[7] M. Gochfeld, Cases of mercury exposure, bioavailability, and absorption, Ecotoxicol. Environ. Saf. 56 (2003) 174–179.
[8] H. Huang, Y. Weng, L. Zheng, B. Yao, W. Weng, X. Lin, Nitrogen-doped carbon quantum dots as fluorescent probe for "off-on" detection of mercury ions, L-cysteine and iodide ions, J. Colloid Interface Sci. 506 (2017) 373–378.
[9] M. Tuzen, I. Karaman, D. Citak, M. Soylak, Mercury(II) and methyl mercury determinations in water and fish samples by using solid phase extraction and cold vapour atomic absorption spectrometry combination, Food Chem. Toxicol. 47 (2009) 1648–1652.
[10] G. Genchi, M. Sinicropi, A. Carocci, G. Lauria, A. Catalano, Mercury exposure and heart diseases, Int. J. Environ. Res. Publ. Health 74 (2017) 1–13.
[11] S. Díez, Human health effects of methylmercury exposure, Rev. Environ. Contam. Toxicol. 198 (2009) 111–125.
[12] Y. Hong, Y. Kim, K. Lee, Methylmercury exposure and health effects, J. Prev. Med. Publ. Health 45 (2012) 353–363.
[13] Y. Zhang, Y.H. He, P.P. Cui, X.T. Feng, L. Chen, Y.Z. Yang, X.G. Liu, Water-soluble, nitrogen-doped fluorescent carbon dots for highly sensitive and selective detection of Hg2+ in aqueous solution, Roy. Soc. Chem 5 (2015) 40393–40401.
[14] H. Erxleben, Jaromir Ruzicka, Atomic absorption spectroscopy for mercury, automated by sequential injection and miniaturized in lab-on-valve system, Anal. Chem. 77 (2005) 5124–5128.
[15] Y. Chen, L. Wu, Y. Chen, N. Bi, X. Zheng, H. Qi, M. Qin, X. Liao, H. Zhang, Y. Tian, Determination of mercury(II) by surface-enhanced Raman scattering spectroscopy based on thiol-functionalized silver nanoparticles, Microchim. Acta 177 (2012) 341–348.
[16] K. Srinivasan, K. Subramanian, K. Murugan, K. Dinakaran, Sensitive fluorescence detection of mercury(II) in aqueous solution by the fluorescence quenching effect of MoS_2 with DNA functionalized carbon dots, Analyst 141 (2016) 6344–6352.
[17] D. Nixon, M. Burritt, T. Moyer, The determination of mercury in whole blood and urine by inductively coupled plasma mass spectrometry, Spectrochim. Acta B Atom Spectrosc. 54 (1999) 1141–1153.
[18] Y. Wang, F. Yang, X. Yang, Colorimetric detection of mercury(II) ion using unmodified silver nanoparticles and mercury-specific oligonucleotides, ACS Appl. Mater. Interfaces 2 (2010) 339–342.
[19] K. Bera, A. Das, M. Nag, S. Basak, Development of a Rhodamine−Rhodanine-based fluorescent mercury sensor and its use to monitor real-time uptake and distribution of inorganic mercury in live zebrafish larvae, Anal. Chem. 86 (2014) 2740–2746.
[20] L. Li, B. Yu, T. You, Nitrogen and sulfur co-doped carbon dots for highly selective and sensitive detection of Hg (II) ions, Biosens. Bioelectron. 74 (2015) 263–269.
[21] J. Hua, J. Yang, Y. Zhu, C. Zhao, Y. Yang, Highly fluorescent carbon quantum dots as nanoprobes for sensitive and selective determination of mercury (II) in surface waters, Spectrochim. Acta Part A Mol. Biomol. Spectrosc. 187 (2017) 149–155.
[22] Y. Ma, Z. Zhang, Y. Xu, M. Ma, B. Chen, L. Wei, L. Xiao, A bright carbon-dot-based fluorescent probe for selective and sensitive detection of mercury ions, Talanta 161 (2016) 476–481.
[23] Q. Xu, P. Pu, J. Zhao, C. Dong, C. Gao, Y. Chen, J. Chen, Y. Liua, H. Zhou, Preparation of highly photoluminescent sulfur-doped carbon dots for Fe(iii) detection, J. Mater. Chem. A 3 (2015) 542–546.
[24] C. Zhao, Y. Jiao, J. Hua, J. Yang, Y. Yang, Hydrothermal synthesis of nitrogen-doped carbon quantum dots as fluorescent probes for the detection of dopamine, J. Fluoresc. 28 (2018) 269–276.
[25] K. Jiang, S. Sun, L. Zhang, Y. Lu, A. Wu, C. Cai, H. Lin, Red, green, and blue luminescence by carbon dots: full-color emission tuning and multicolor cellular imaging, Angew. Chem. 54 (2015) 1–5.
[26] X. Cui, Y. Wang, J. Liu, Q. Yang, B. Zhang, Y. Gao, Y. Wang, Dual functional N- and S-co-doped carbon dots as the sensor for temperature and Fe^{3+} ions, Sensor. Actuator. B Chem. 242 (2017) 1272–1280.
[27] R. Atchudan, T. Edison, K. Aseer, S. Perumal, N. Karthik, Y. Lee, Highly fluorescent nitrogen-doped carbon dots derived from Phyllanthus acidus utilized as a fluorescent probe for label-free selective detection of Fe^{3+} ions, live cell imaging and fluorescent ink, Biosens. Bioelectron. 99 (2018) 303–311.
[28] H. Wang, Q. Lu, M. Li, H. Li, Y. Liu, H. Li, Y. Zhang, S. Yao, Electrochemically prepared oxygen and sulfur co-doped graphitic carbon nitride quantum dots for fluorescence determination of copper and silver ions and biothiols, Anal. Chim. Acta 1027 (2018) 121–129.
[29] Y. Wang, W. Wua, M. Wu, H. Sun, H. Xie, C. Hu, X. Wu, J. Qiu, Yellow-visual fluorescent carbon quantum dots from petroleum coke for the efficient detection of Cu^{2+} ions, N. Carbon Mater. 30 (2015) 550–559.
[30] M. Zan, L. Rao, H. Huang, W. Xie, D. Zhu, L. Li, X. Qie, S. Guo, X. Zhao, W. Liu, W. Dong, A strong green fluorescent nanoprobe for highly sensitive and selective detection of nitrite ions based on phosphorus and nitrogen co-doped carbon quantum dots, Sensor. Actuator. B Chem. 262 (2018) 555–561.
[31] M. Tuerhong, X. Yang, Y. Bo, Review on carbon dots and their applications, Chin. J. Anal. Chem. 45 (2017) 139–150.
[32] Y. Xu, J. Liu, C. Gao, E. Wang, Applications of carbon quantum dots in electrochemiluminescence: a mini review, Electrochem. Commun. 48 (2014) 151–154.
[33] J. da Silva, H. Gonc¸alves, Analytical and bioanalytical applications of carbon dots, Trends Anal. Chem. 30 (2011) 1327–1336.
[34] A. Chandra, N. Singh, Biocompatible fluorescent carbon dots for ratiometric intracellular pH sensing, Chemistry Select 2 (2017) 5723–5728.
[35] M. Yang, B. Li, K. Zhong, Y. Lu, Photoluminescence properties of N-doped carbon dots prepared in different solvents and applications in pH sensing, J. Mater. Sci. 53 (2018) 2424–2433.
[36] D. Zhong, H. Miao, K. Yang, X. Yang, Carbon dots originated from carnation for fluorescent and colorimetric pH sensing, Mater. Lett. 166 (2016) 89–92.
[37] Y. Zhang, Y. Wang, X. Feng, F. Zhang, Y. Yang X. Liu, Effect of reaction temperature on structure and fluorescence properties of nitrogen-doped carbon dots, Appl. Surf. Sci. 387 (2016) 1236–1246.
[38] Y. Liu, Q. Zhou, Sensitive pH probe developed with water-soluble fluorescent carbon dots from chocolate by one step hydrothermal method, Int. J. Environ. Anal. Chem. 97 (2017) 1119–1131.
[39] R. Liu, D. Wu, X. Feng, K. Mulllen, Bottom-up fabrication of photoluminescent graphene quantum dots with uniform morphology, J. Am. Chem. Soc. 133 (2011) 15221–15223. .
[40] S. Sagbas, N. Sahiner, "Carbon Dots: Preparation, Properties, and Application" Chapter 22 in "Nanocarbon and its Composites", 2019, pp. 651–676. .
[41] E. Yahyazadeh, F. ShemIrani, Easily synthesized carbon dots for determination of mercury (II) in water samples, Heliyon 5 (2019) e01596.
[42] X. Li, S. Zhang, S. Kulinich, Y. Liu, H. Zeng, Engineering surface states of carbon dots to achieve controllable luminescence for solid-luminescent composites and sensitive Be^{2+} detection, Sci. Rep. 4 (2014) 4976.
[43] Z. Yan, J. Shu, Y. Yu, Z. Zhang, Z. Liu J. Chen, Preparation of carbon quantum dots based on starch and their spectral properties, Luminescence 30 (2014) 388–392.
[44] Y. Song, S. Zhu, S. Zhang, Y. Fu, L. Wang, X. Zhao, B. Yang, Investigation from chemical structure to photoluminescent mechanism: a type of carbon dots from the pyrolysis of citric acid and an amine, J. Mater. Chem. C 3 (2015) 5976–5984.
[45] L. Li, X. Jiao, Y. Zhang, C. Cheng, K. Huang, L. Xu, Green synthesis of fluorescent carbon dots from Hongcaitai for selective detection of hypochlorite and mercuric ions and cell imaging, Sensor. Actuator. B Chem. 263 (2018) 426–435.
[46] Y. Zhang, N. Jing, J. Zhang, Y. Wang, Hydrothermal synthesis of nitrogen-doped carbon dots as a sensitive fluorescent probe for the rapid, selective determination of Hg^{2+}, Int. J. Environ. Anal. Chem. 97 (2017) 841–853.
[47] Z. Feng, Z. Li, X. Zhang, Y. Shi, N. Zhou, Nitrogen-doped carbon quantum dots as fluorescent probes for sensitive and selective detection of nitrite, Molecules 22 (2017) 2061.
[48] H. Ding, J. Wei, H. Xiong, Nitrogen and sulfur co-doped carbon dots with strong blue luminescence, Nanoscale 6 (2014) 13817–13823.
[49] C. Zhang, Y. Cui, L. Song, X. Liu, Z. Hu, Microwave assisted one-pot synthesis of graphene quantum dots as highly sensitive fluorescent probes for detection of iron ions and pH value, Talanta 150 (2016) 54–60.
[50] Q. Hua, M. Paau, Y. Zhang, W. Chan, X. Gong, L. Zhang, M. Choi, Capillary electrophoretic study of amine/carboxylic acid-functionalized carbon nanodots, J. Chromatogr. A 1304 (2013) 234–240.
[51] M.S. Dresselhaus, A. Jorio, M. Hofmann, G> Dresselhau, R. Saito, Perspectives on carbon nanotubes and graphene Raman spectroscopy, Nano Lett. 10 (3) (2010) 751–758.
[52] S. Kumara, A.K. Ojha, B. Ahmed, A. Kumara, J. Das, A. Materny, Tunable (violet to green) emission by high-yield graphene quantum dots and exploiting its unique properties towards sun-light-driven photocatalysis and supercapacitor electrode materials, Mater. Today Commun. 11 (2017) 76–86.
[53] Y. Hu, J. Yang, J. Tian, J.S. Yu, How do nitrogen-doped carbon dots generate from molecular precursors? An investigation of the formation mechanism and a solution-based large-scale synthesis, J. Mater. Chem. B 3 (27) (2015) 5608–5614. .
[54] A. Mewada, S. Pandey, S. Shinde, N. Mishra, G. Oza, M. Thakur, M. Sharon, M. Sharon, Green synthesis of biocompatible carbon dots using aqueous extract of Trapa bispinosa peel, Mater. Sci. Eng. C 33 (2013) 2914–2917.
[55] A.C. Ferrari, Raman spectroscopy of graphene and graphite: disorder, electron–phonon coupling, doping and nonadiabatic effects, Solid State Commun. 143 (2007) 47–57.
[56] X. Meng, Y. Wang, X. Liu, M. Wang, Y. Zhan, Y. Liu, W. Zhu, W. Zhang, L. Shi, X. Fang, Supramolecular nanodots derived from citric acid and beta-amines with high quantum yield and sensitive photoluminescence, Opt. Mater. 77 (2018) 48–54.
[57] C.H. Lei, X.E. Zhao, S.L. Jiao, a L. He, Y. Li, a S.Y. Zhua, J.M. You, A turn-on fluorescent sensor for detection of melamine based on the anti-quenching ability of Hg^{2+} to carbon nanodots, Analy. Methods 8 (2016) 4438–4444.
[58] H. Huang, J. Lv, D. Zhou, N. Bao, Y. Xu, A. Wang, J. Feng, One-pot green synthesis of nitrogen-doped carbon nanoparticles as fluorescent probes for mercury ions, RSC Adv. 3 (2013) 21691–21696.
[59] Y. Liu, C. Liu, Z. Zhang, Synthesis of highly luminescent graphitized carbon dots and the application in the Hg^{2+} detection, Appl. Surf. Sci. 263 (2012) 481–485.
[60] Z. Qian, J. Ma, X. Shan, H. Feng, L. Shao, J. Chen, Highly luminescent N-doped carbon quantum dots as an effective multifunctional fluorescence sensing platform, Chem. A. Eur J. 20 (2014) 2254–2263.

[61] K.H. Hama Aziz, K.M. Omer, R.F. Hamarawf, Lowering the detection limit towards nanomolar mercury ion detection via surface modification of N-doped carbon quantum dots, New J. Chem. 43 (2019) 8677–8683.
[62] J. He, H. Zhang, J. Zou, Y. Liu, J. Zhuang, Y. Xiao, B. Lei, Carbon dots-based fluorescent probe for "off-on" sensing of Hg(II) and I^-, Biosens. Bioelectron. 79 (2016) 531–535.
[63] P. Roy, P. Chen, A.P. Periasamy, Y. Chen, H. Chang, Photoluminescent carbon nanodots: synthesis, physicochemical properties and analytical applications, Mater. Today 18 (2015) 447–458.
[64] Z. Li, Y. Wang, Y. Ni, S. Kokot, A rapid and label-free dual detection of Hg (II) and cysteine with the use of fluorescence switching of graphene quantum dots, Sensor. Actuator. B Chem. 207 (2015) 490–497.
[65] N. Thi, N. Anh, A.D. Chowdhury, R. Doong, Highly sensitive and selective detection of mercury ions using N, S-codoped graphene quantum dots and its paper strip based sensing application in wastewater, Sensor. Actuator. B Chem. 252 (2017) 1169–1178.
[66] G. Ren, Y. Meng, Q. Zhang, M. Tang, B. Zhu, F. Chai, C. Wang, Z. Su, Nitrogen-doped carbon dots for the detection of mercury ions in living cells and visualization of latent fingerprints, New J. Chem. 42 (2018) 6824–6830.
[67] K. Patir, S.K. Gogol, Nitrogen-doped carbon dots as fluorescence ON–OFF–ON sensor for parallel detection of copper (ii) and mercury (ii) ions in solutions as well as in filter paper-based microfluidic device, Nanoscale Adv. 2 (2019) 592–601. .
[68] N. Martins, J. Ângelo, A.V. Girão, T. Trindade, L. Andrade, A. Mendes, N-doped carbon quantum dots/TiO_2 composite with improved photocatalytic activity, Appl. Catal. B Environ. 193 (2016) 67–74.